Soft Matter

PAPER

View Article Online
View Journal | View Issue

CrossMark click for updates

Cite this: *Soft Matter*, 2014, **10**, 8202

Wet adhesion between two soft layers

Kai Li[a] and Shengqiang Cai*[b]

Received 6th July 2014
Accepted 4th August 2014

DOI: 10.1039/c4sm01470g

www.rsc.org/softmatter

Two solids can adhere to each other in the presence of a liquid bridge between them, which is called wet adhesion. When the solid is soft, the liquid bridge can cause deformation in the material, and in turn, the deformation may have dramatic effects on the wet adhesion. To investigate the effect, in this article, we calculate the deformation in two soft layers with different separations and connected by a liquid bridge. We illustrate the effect of deformation in the soft layers on the adhesive force. For a given liquid volume and separation between the two layers, the adhesive force increases dramatically by decreasing the elastic moduli of the soft layers. We also discuss the contact between the two soft layers due to the deformation caused by the liquid bridge. Depending on the volume of the liquid bridge, the two layers may be in contact with each other at the center of the wetting area or some other locations between the center and the contact line. The results may improve current understanding of wet adhesion between soft materials and have potential applications in designing and fabricating soft devices and structures.

Introduction

Adhesion between two solid surfaces can be vital in making various structures and devices.[1–3] In terms of the adhesive mechanism, adhesion between two solids can be broadly divided into dry adhesion and wet adhesion. For dry adhesion, intermolecular interaction such as van der Waals force is responsible for the adhesion.[4,5] Many animals, including insects, spiders, lizards and geckos, have the capability to cling to different surfaces using van der Waals forces.[6,7] For wet adhesion, liquid bridges exist between two adjacent surfaces and capillary force is responsible for the adhesion.[8,9] Examples of wet adhesion range from the aggregation of granular materials in a wet environment[10] and crack propagation in the presence of moisture,[11] to the attachment of animals like beetles, blowflies and ants, which can release fluid to attach their pads onto different surfaces.[12–14]

Many experiments have shown that adhesion can cause deformation in the material, which, in turn, can dramatically affect the adhesion properties.[15–17] In the past, deformation in the material due to dry adhesion has been intensively studied.[18,19] For example, based on London theory of van der Waals forces between small particles and colloids,[20] Johnson–Kendall–Roberts (JKR) theory extended the Hertz contact theory[21] to study the adhesion between two elastic spheres, with considering the deformation caused by van der Waals forces.[22] Gao *et al.* proposed an accordion model to investigate the properties of gecko adhesion, and found that deformation in a foldable hard skin due to dry adhesion is crucial for the multi-functionalities of the accordion pad including self-cleaning, strong attachment and easy detachment.[23] Diverse deformation modes and mechanical instabilities, such as cavitation and elastic fingering, have been frequently observed in the process of separating a rigid probe from the surface of a soft adhesive thin film.[24–26] It has been clearly demonstrated that complex deformations in the materials are closely related to their adhesion properties.[24–26]

Compared to dry adhesion, the deformation in the material due to capillary forces in wet adhesion has been much less studied. This is probably because the deformation in the material caused by capillary force is usually small and negligible. However, recent experiments have shown that capillary forces can induce large deformations or even mechanical instabilities in soft materials.[27–29]

As a matter of fact, the deformation in the material due to capillary force can be estimated by comparing the size of the material with elasto-capillary length: γ/E, where E is the elastic modulus of the material and γ is the surface free energy density.[30] When the size of the material is much larger than the elasto-capillary length, capillarity-induced deformation can be ignored in the material. However, when the size of the material is comparable or smaller than the elasto-capillary length, capillarity-induced deformation in the material can be dramatic.[31,32] Therefore, in this paper, we study wet adhesion between two soft layers with considering the deformation of the material.

In calculating the deformation of a solid caused by a liquid droplet, the analysis of the deformation around a three-phase contact line is critical. To avoid possible deformation singularity in the three-phase contact line, surface stresses in the solid[33,34] are considered. By closely following the methods in the

[a]*Department of Civil Engineering, Anhui Jianzhu University, Hefei, Anhui 230601, P R China*

[b]*Department of Mechanical and Aerospace Engineering, University of California, San Diego, La Jolla, CA 92093, USA. E-mail: shqcai@ucsd.edu*

literature,[35] we calculate the deformation of the soft layers caused by the liquid bridge connecting them. Using the shooting method, for a given liquid volume and separation between two layers, we calculate the adhesive force caused by the liquid bridge. The influence of elastic moduli of soft layers on the adhesive force is also investigated. The results may improve current understanding of wet adhesion in soft materials and have potential applications in designing and fabricating soft devices and structures.

Model and formulation

Fig. 1a sketches the system to be investigated in this article. Two identical soft layers, with infinitely large lengths in two planar directions and finite thickness h, are in wet adhesion with each other through a liquid bridge with volume V. The two layers are attached to two rigid plates respectively. Two separation forces with equal magnitudes but opposite directions are applied on the rigid plates. We assume that the shape of the liquid bridge is axisymmetric with radius R of wetting area on the top and bottom of the soft layers, as shown in Fig. 1a. We specify a cylindrical coordinate system, whose origin O lies on the surface of the undeformed lower soft layer (Fig. 1a).

Due to the presence of liquid surface tension, the pressure inside the liquid bridge is different from the pressure outside, and the difference is defined as Laplace pressure P, which can be calculated by the Young–Laplace equation,[36]

$$P = \gamma_{lg}\left(\frac{1}{R_1} + \frac{1}{R_2}\right) \quad (1)$$

where R_1 and R_2 are the two principle radii of curvature of the surface of the liquid bridge as shown in Fig. 1a, and γ_{lg} is the surface tension of the liquid. Since the effect of gravity is neglected, P is the constant in the liquid bridge, and the surface of the liquid bridge has the same mean curvature at any point.

The contact angle θ_0 of the liquid bridge on the layer is given by Young's equation,[36]

$$\gamma_{sg} - \gamma_{sl} = \gamma_{lg}\cos\theta_0 \quad (2)$$

where γ_{sl} and γ_{sg} are the solid–liquid interfacial free energy density and solid–gas interfacial free energy density, respectively. Eqn (2) is the consequence of minimizing total interfacial free energy of the system with allowing the contact line move freely in the tangential direction of the surface. However, eqn (2) leads to an imbalance of vertical forces with magnitude $\gamma_{lg}\sin\theta_0$ (Fig. 1b), which can deform the soft layers as well.

When the system is in equilibrium, the separation force F is balanced with the adhesive force which is the sum of the effect of liquid surface tension and Laplace pressure P as shown in Fig. 1c:

$$F = 2\pi R\gamma_{lg}\sin\theta_0\cos(\theta - \theta_0) + \pi R^2 P \quad (3)$$

where θ is commonly known as the "apparent" contact angle, which is the angle between the surface of the liquid bridge at the contacting point and the horizontal surface as shown in Fig. 1b.

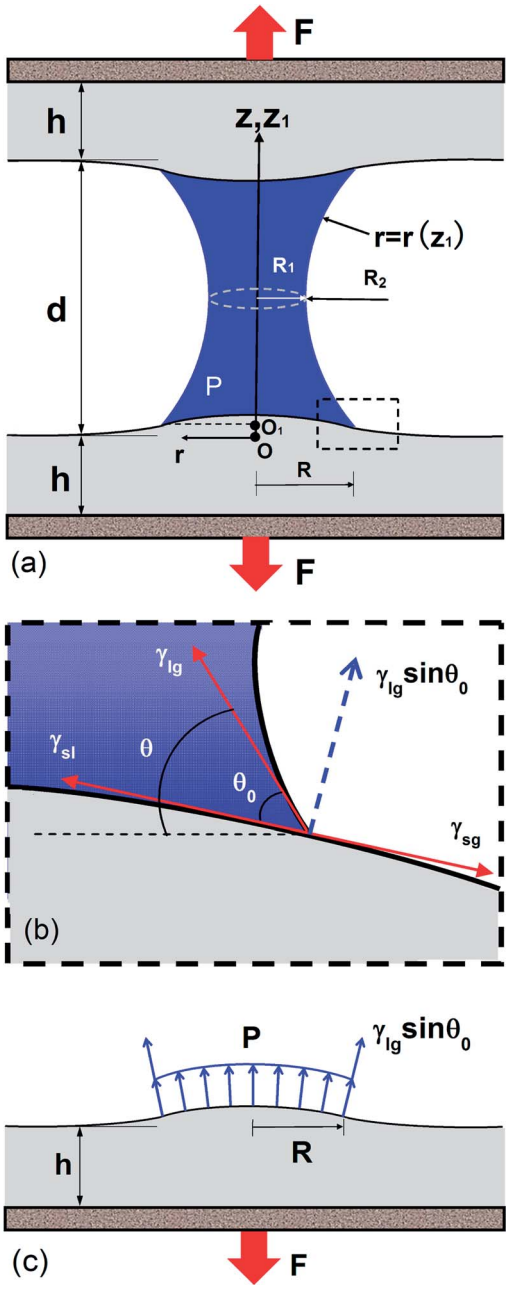

Fig. 1 (a) Schematic of a liquid bridge connecting two soft layers. (b) Young's equation leads to a net force with magnitude $\gamma_{lg}\sin\theta_0$ per unit length at the contact line. (c) The soft layer deforms under the action of the Laplace pressure and liquid surface tension. In this case, the Laplace pressure P always pulls the soft layer because the pressure inside the liquid is smaller than the atmospheric pressure.

To obtain the Laplace pressure in eqn (3), we need to calculate the profile of the liquid bridge for a given volume and separation between two layers. To describe the profile of the liquid bridge affected by surface deformation of layers, we set up a new vertical coordinate as $z_1 = z - u_z(R, 0)$, where $u_z(R, 0)$ is the vertical displacement of the soft layer at the contact line. The shape of the liquid bridge can be described by the function

$r = r(z_1)$ (Fig. 1a), and the two principle radii of curvature are given by $R_1 = -r\sqrt{1+r'^2}$, $R_2 = (1+r'^2)^{3/2}/r''$. So, the Young–Laplace equation in eqn (1) can be rewritten as

$$\frac{P}{\gamma_{lg}} = \frac{r''}{(1+r'^2)^{3/2}} - \frac{1}{r\sqrt{1+r'^2}}. \quad (4)$$

The boundary conditions for eqn (4) are

$$r|_{z1=0} = R \quad (5a)$$

$$r'|_{z1=0} = -1/\tan\theta. \quad (5b)$$

Because of the mirror symmetry, we have,

$$r'|_{z1=d/2-uz(R,0)} = 0. \quad (6)$$

Ignoring the deformation of the two soft layers, the above equations are adequate to compute the Laplace pressure and the adhesive force. However, as discussed in the Introduction, in this article we intend to take into account the deformation of the soft layers caused by the liquid bridge and investigate the effect of the softness of the layers on the wet adhesion. In the following section, we are going to list the equations for calculating the deformation in the soft layers.

Because the shape of the liquid bridge is assumed to be axisymmetric, the deformation of the soft layers is also axisymmetric. We assume both strain field and rotation in the material are small, so the governing equations for the axisymmetric deformation of soft layers are the Navier equations,[37]

$$(1-2\nu)\left(\nabla^2 u_r - \frac{u_r}{r^2}\right) + \frac{\partial}{\partial r}(\nabla\cdot\mathbf{u}) = 0 \quad (7a)$$

$$(1-2\nu)\nabla^2 u_z + \frac{\partial}{\partial z}(\nabla\cdot\mathbf{u}) = 0 \quad (7b)$$

where u_r and u_z are the r and z components of the displacement $\mathbf{u}$, and ν is the Poisson ratio of the material. In this article, strains in deformed soft layers do not exceed 8% in all the calculations. Although 8% strain is by no means infinitesimal deformation, we believe that linear elasticity can still be a good approximation in our model. As a matter of fact, linear theories have met with remarkable success in describing even moderately large deformation.

Because the two soft layers are identical, we only need to calculate the deformation in the bottom layer. The layer is constrained by a rigid plate on its bottom surface, so the boundary condition for the displacement is

$$\mathbf{u}(r, -h) = 0 \quad (8)$$

for all r with origin O.

The traction imposed by the liquid bridge on the surface of the soft layer in vertical direction is given by

$$\sigma_{zz}(r, 0) = \gamma_{lg}\sin\theta_0\cos(\theta-\theta_0)\delta(R-r) + PH(R-r) \quad (9)$$

for all r with origin O, where $\delta(x)$ and $H(x)$ are the Dirac delta and Heaviside step functions, respectively. It is noted that the angle θ can be affected by the deformation of the soft layer, as

$$\theta = \theta_0 - \arctan\left(\frac{\partial u_z(R,0)}{\partial r}\right). \quad (10)$$

To solve the axisymmetric problem, we follow the method adopted by Jerison *et al.*[35] Because the tangential traction on the surface $\sigma_{zr}(r, 0)$ is negligible, we assume that the deformation of the soft layer is only caused by the vertical traction $\sigma_{zz}(r, 0)$. The surface displacement of the soft layer is given by[35]

$$u_z(r, 0) = \mathbf{H}_0^{-1}[K_{zz}^{-1}(s)\mathbf{H}_0[\sigma_{zz}(r, 0)]] \quad (11)$$

where $\mathbf{H}_0$ is the Hankel transformation of order 0, and $K_{zz}^{-1}(s)$ is[35]

$$K_{zz}^{-1}(s) = \frac{2(1-\nu^2)}{sE}\frac{1}{\frac{5-12\nu+8\nu^2+2s^2h^2+(3-4\nu)\cosh(2sh)}{(3-4\nu)\sinh(2sh)-2sh} + \frac{2s(1-\nu^2)\gamma_s}{E}} \quad (12)$$

where s is the radial wavenumber of the Hankel transform of order 0, and the surface stress of the soft layers γ_s is considered here for cutting off the divergence of strain at the triple line. For simplicity, we assume that surface stress is the same on the solid–liquid interface and solid–gas interface. The deformation can be obtained by a dual integral equation when the surface stresses on the solid–liquid interface and solid–gas interface are different.[38] In the following calculations, we set the ratio between solid–liquid interfacial free energy density and surface stress of the soft layer as $\gamma_{lg}/\gamma_s = 0.5$.

Combining eqn (9) and (11), we can obtain the vertical displacement of the soft layer on the surface caused by the liquid bridge as

$$u_z(r,0) = \int_0^\infty s\left[\gamma_{lg}\sin\theta_0\cos(\theta-\theta_0)RJ_0(sR) + \frac{PRJ_1(sR)}{s}\right]K_{zz}^{-1}(s)J_0(sr)\mathrm{d}s \quad (13)$$

where the expression within the square of the integration is the Hankel transform of order 0 of the right-hand side of eqn (9), J_0 and J_1 are the 0 and 1 order Bessel function of the first kind respectively.

Based on the displacement given in eqn (13), we can calculate the volume of the liquid bridge by the integration,

$$V = 2\int_0^{d/2-u_z(R,0)} \pi r^2 \mathrm{d}z_1 - 2\int_0^R 2\pi r[u_z(r,0) - u_z(R,0)]\mathrm{d}r, \quad (14)$$

where the first term of the right-hand side is the volume enclosed by the outline of the liquid bridge $r = r(z_1)$ and two horizontal axes $z_1 = 0$ and $z_1 = d - 2u_z(R, 0)$, and the second term corresponds to the volume of the soft layers above $z_1 = 0$ and below $z_1 = d - 2u_z(R, 0)$.

In the following section, we are going to describe the numerical method of solving the above equations and discuss the results we obtain.

Results and discussion

For a given volume of the liquid bridge, to calculate the adhesive force as a function of the separation between two layers, we use the shooting method. In the calculation, we first assume the values of radius R of the wetting area and Laplace pressure P, and calculate surface deformation by solving eqn (13) with the corresponding boundary conditions. After the surface deformation is computed, we further calculate the liquid profile by solving eqn (4) with the corresponding boundary conditions eqn (5a) and (5b). Based on the surface deformation and liquid profile, we can calculate the separation d and liquid volume V, by solving eqn (6) and (14), respectively. Through several iterations, we can obtain the contacting radius and Laplace pressure for prescribed liquid volume V and separation d. After the radius of the wetting area R and the Laplace pressure P are calculated, we derive the adhesive force between the two soft layers for a given liquid volume V and separation d from eqn (3). In the calculation, we assume that the soft layer is incompressible, *i.e.*, $\nu = 0.5$, and the contacting angle $\theta_0 = \pi/3$.

Fig. 2 plots the adhesive force as a function of separation d for several elastic moduli of the soft layers and different volumes of liquid bridge. Because the radius of the wetting area R and the Laplace pressure P decreases with increasing separation d, the adhesive force decreases monotonically with increasing the separation. From Fig. 2a–c, we can also conclude that larger volume of liquid bridge results in larger adhesive force for the same separation distance between the two layers.

Fig. 2 also illustrates that the separation force is larger for softer layers with the same separation distance between the two layers. To better show the influence of softness of the layer on the magnitude of adhesive force, Fig. 3 plots the adhesive force as a function of modulus of the soft layer for three different volumes of liquid. It clearly shows that the adhesive force can dramatically increase when the layer is soft. For instance, with the liquid volume $V/h^3 = 0.3$ and the separation $d/h = 0.359$, the adhesive force can increase as large as 4 times when the non-dimensional number γ_{lg}/Eh changes from 0.01 to 0.08.

If the separation between two layers is too large, the liquid bridge breaks, which can be predicted by instability analysis on the liquid.[39,40] In this paper, because we focus on the effect of the elastic modulus of the soft layer, we stop our calculation of the force-separation curve once the Laplace pressure becomes zero, which is actually very close to the breakage of the liquid bridge.

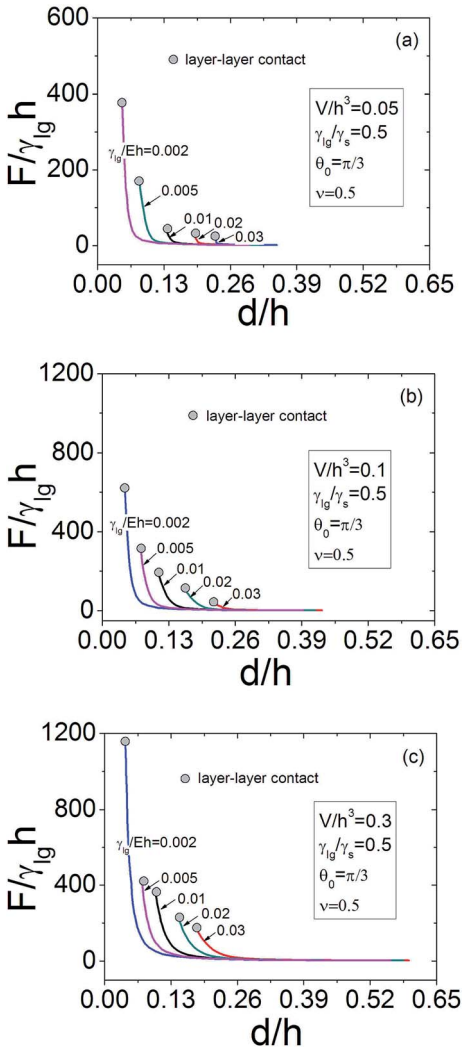

Fig. 2 Adhesive force between two soft layers as a function of separation distance for different elastic moduli of the soft layers with three different volumes of the liquid bridge: (a) $V/h^3 = 0.05$; (b) $V/h^3 = 0.1$; (c) $V/h^3 = 0.3$. To avoid the complexity of calculating contact between the two layers, calculations start from a separation distance larger than the distance for the initial contact, which is marked as grey circular dots in the figure.

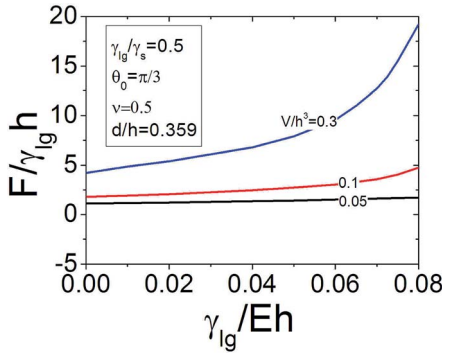

Fig. 3 Adhesive force between the two soft layers increases with decreasing the elastic moduli of the soft layers.

If the separation between the two layers is too small, under the action of surface tension and Laplace pressure, the surfaces of the two soft layers can deform and come into contact with each other. To avoid the complexity of calculating contact, our calculation starts from the separation distance larger than the distance when the contact between the two soft layers initially happens. The circular solid points in Fig. 2 indicate the conditions when two surfaces of the layers initially come into contact with each other.

Fig. 4 plots how the elastic modulus affects the contact between the two soft layers, for different volumes of liquid bridge. The layers with a lower modulus can be in contact with each other for a larger separation distance. However, the separation distance between the two layers for the initial contact does not necessarily change monotonically with increasing liquid volume, as shown in Fig. 4. For $\gamma_{lg}/Eh = 0.1$, the separation distance for initial contact with $V/h^3 = 0.3$ is smaller than that with smaller volume, $V/h^3 = 0.1$. Interestingly, the separation distance for initial contact with $V/h^3 = 0.05$ is also smaller than that with $V/h^3 = 0.1$.

Fig. 5 plots the mean curvature of the liquid bridge as a function of separation, for different liquid volumes. For a fixed elastic modulus of the soft layer, mean curvature of the surface of the liquid bridge decreases with increasing the separation. For a given separation, the mean curvature of the liquid bridge increases with decreasing elastic modulus. The result implies that soft layers tend to increase the Laplace pressure in the liquid bridge. We can understand the results as follows: for a fixed liquid volume and separation, the surfaces of the two layers with smaller elastic modulus are closer to each other through larger surface deformation. Therefore, for softer layers, the mean curvature of the liquid bridge and the Laplace pressure in the liquid are larger.

Fig. 6a and b plot the displacement of the wetting area of the soft layer for several separation distances, with liquid volumes $V/h^3 = 0.05$ and $V/h^3 = 0.1$, respectively. For $V/h^3 = 0.05$ (Fig. 6a), when the separation is large, the maximum vertical displacement of the soft layer is at the contact line, *i.e.* $r/R = 1$. When the separation is small, the maximum displacement is at the center, *i.e.* $r/R = 0$. Therefore, when the two soft layers get close enough, they come into contact with each other at the center first. For $V/h^3 = 0.1$ (Fig. 6b), when the separation is large, the maximum displacement is also at the contact line. However, when the separation decreases, the maximum displacement moves to the center of the contacting area. When the separation becomes small enough, the maximum displacement appears at a location between the center and the contact line. In consequence, when the two soft layers get close enough, they first come into contact with each other at certain location between the contact line and the center of the wetting area.

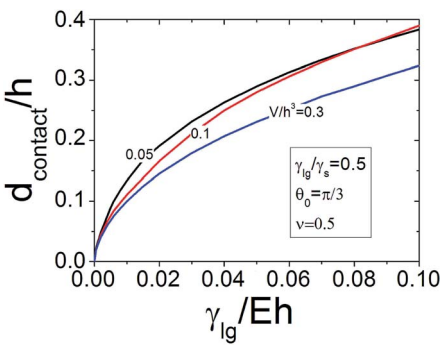

Fig. 4 Dependence of separation distance for the initial contact between the two soft layers on their elastic moduli, for three different volumes of liquid bridge.

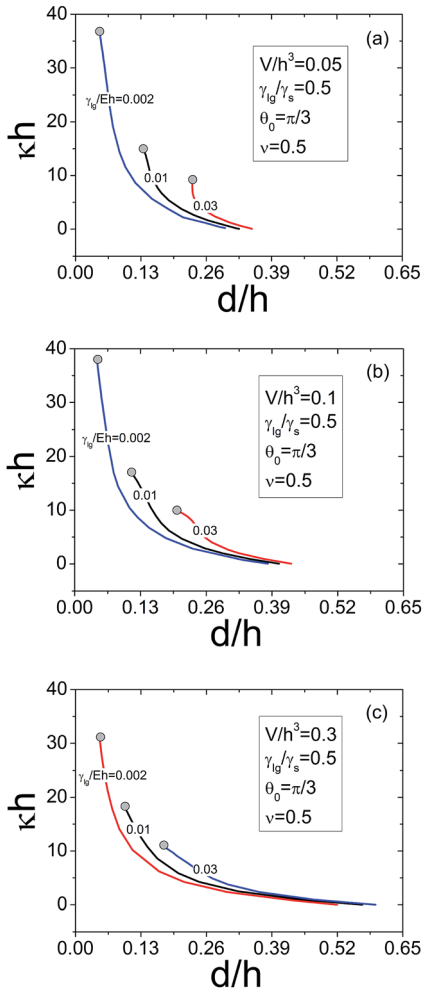

Fig. 5 Mean curvature of the liquid bridge surface, which is defined as $k = 1/R_1 + 1/R_2$, decreases with the increase of the separation between the two soft layers for three different liquid bridge volumes: (a) $V/h^3 = 0.05$, (b) $V/h^3 = 0.1$, (c) $V/h^3 = 0.3$.

As shown in Fig. 1c and eqn (3), the deformation in the soft layer is induced by the surface tension and Laplace pressure. The surface tension acts on the contact line, thereby generating the largest vertical displacement at the contact line. However the Laplace pressure induces the largest vertical displacement at the center of the wetting area, when the radius of the wetting area is small. The Laplace pressure can cause the largest vertical displacement at a location apart from the center, when the wetting area is large. The deformation shown in Fig. 6a and b is due to the combination of surface tension and Laplace pressure.

Fig. 6c plots vertical displacement at the center of the wetting area as a function of the separation. For $V/h^3 = 0.05$, the vertical

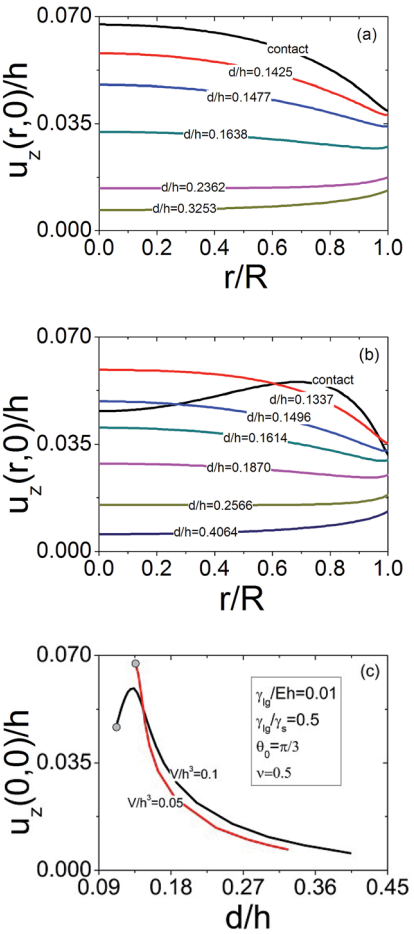

Fig. 6 Vertical displacement of the wetting area of the soft layers for different separation distances with contact angle $\theta_0 = \pi/3$ and two different volumes of the liquid bridge: (a) $V/h^3 = 0.05$ and (b) $V/h^3 = 0.1$. (c) Plots vertical displacement at the center of the wetting area of the soft layer as a function of the separation, with two different volumes of the liquid bridge $V/h^3 = 0.05$ and $V/h^3 = 0.1$.

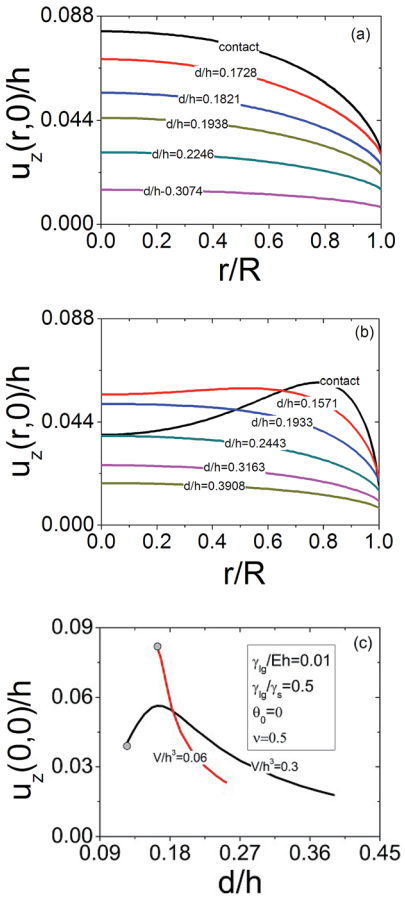

Fig. 7 Vertical displacement of the wetting area for different separation distances with zero contact angle $\theta_0 = 0$ and two different volumes of the liquid bridge: (a) $V/h^3 = 0.06$, (b) $V/h^3 = 0.3$. (c) Plots vertical displacement at the center of the wetting area of the soft layer as a function of the separation, with two different volumes of the liquid bridge $V/h^3 = 0.3$ and $V/h^3 = 0.06$.

displacement at the center is a monotonic function of the separation. For $V/h^3 = 0.1$, the vertical displacement at the center is a non-monotonic function of the separation. To be more detailed, the vertical displacement at the center of the soft layer increases first and then decreases with increasing the separation. The non-monotonic function can be understood by considering the finite thickness of the soft layer and the Poisson effect of the material. Both Laplace pressure and wetting area decrease with increasing the separation between the two soft layers. Although larger Laplace pressure tends to cause larger vertical displacement at the center, larger wetting area (scaled by the thickness of the soft layer) results in smaller vertical displacement at the center due to Poisson's effect. Therefore, maximal vertical displacement at the center may appear for medium Laplace pressure and wetting area and consequently medium separation as shown in Fig. 6c.

To better illustrate the effect of Laplace pressure on the deformation of the soft layer, we calculate the vertical displacement with assuming the contact angle $\theta_0 = 0$. Therefore, the surface deformation is only induced by the Laplace pressure. Fig. 7a and b plot the displacement for several separations with two different liquid volumes $V/h^3 = 0.06$ and $V/h^3 = 0.3$. When the separation between the two layers is small, for a small liquid volume, the maximal displacement is at the center of the wetting area (Fig. 7a); for a large liquid volume, the peak displacement appears at a location between the center and the contact line (Fig. 7b). Now, however, the maximal vertical displacement of the layers is not at the contact line, even for large separations.

Fig. 7c plots the vertical displacement at the center of the wetting area as a function of the separation. For a small volume $V/h^3 = 0.06$, the vertical displacement at the center is a monotonic function of the separation. For a large volume $V/h^3 = 0.3$, the vertical displacement at the center is a nonmonotonic function of the separation. The result is qualitatively similar to that shown in Fig. 6, though the surface deformation is only induced by the Laplace pressure shown in Fig. 7.

Fig. 8 plots the calculated configuration of two soft layers connected by a liquid bridge with different separations. When the two soft layers are close enough to each other (Fig. 8a), the two soft layers contact at a location between the center and the contact line. With increasing the separation, the radius of the

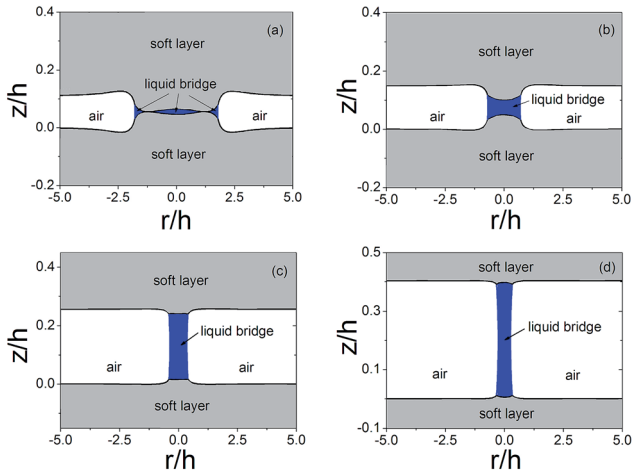

Fig. 8 Snapshots of the deformation of the soft layers and the shape of the liquid bridge at four different separations with the following parameters: $V/h^3 = 0.1$, $\gamma_{lg}/Eh = 0.01$, $\gamma_{lg}/\gamma_s = 0.5$, $\theta_0 = \pi/3$, $\nu = 0.5$. The two layers begin to be in contact with each other when the separation is $d/h = 0.1105$ as shown in (a). The separations are $d/h = 0.1496$ and $d/h = 0.2566$ in (b) and (c) respectively. The Laplace pressure drops to zero when the separation is as large as $d/h = 0.4064$ as shown in (d). It is noted that in the figure, to clearly show the deformation in soft layers, the horizontal scale is selected different from the vertical scale. In addition, only a portion of soft layers are included in the figure. The dimensionless thickness of each soft layer should be 1 and the lateral size of the soft layer is infinitely large.

wetting area and the curvature of the surface of the liquid bridge gradually decrease (Fig. 8b–d). There exists a critical separation between the two layers, beyond which a stable liquid bridge no longer exists due to instability.[39,40]

Conclusions

In this paper, we study wet adhesion between two soft layers connected by a liquid bridge. We calculate the adhesive force between the two soft layers for different separation distances. In the calculation, we have taken into account the surface deformation of the soft layers caused by the liquid bridge. The calculation shows that the adhesive force between two soft layers decreases with increasing separation. For a given liquid volume and separation, the adhesive force caused by the liquid bridge increases with decreasing the elastic moduli of the soft layers. Our calculations have also shown that the two layers may contact each other at small separation. Depending on the volume of the liquid bridge and the moduli of the soft layers, the two soft layers may contact each other at the center of the wetting area or some place between the center and contact line. Our results may improve the understanding of elasto-capillary phenomena in soft materials and have potential applications in designing and fabricating soft devices.

Acknowledgements

Kai Li acknowledges the support from the Anhui Provincial Natural Science Foundation (grant no. 1408085QA18). Shengqiang Cai acknowledges the startup funds from the Jacobs School of Engineering at UCSD.

References

1 H. Lee, B. P. Lee and P. B. Messersmith, *Nature*, 2007, **448**, 338.
2 A. Mahdavi, L. Ferreira, C. Sundback, J. W. Nichol, E. P. Chan, D. J. D. Carter, C. J. Bettinger, S. Patanavanich, L. Chignozha, E. Ben-Joseph, A. Galakatos, H. Pryor, I. Pomerantseva, P. T. Masiakos, W. Faquin, A. Zumbuehl, S. Hong, J. Borenstein, J. Vacanti, R. Langer and J. M. Karp, *Proc. Natl. Acad. Sci.*, 2008, **105**, 2307.
3 E. Arzt, S. Gorb and R. Spolenak, *Proc. Natl. Acad. Sci.*, 2003, **100**, 10603.
4 K. Autumn, M. Sitti, Y. A. Liang, A. M. Peattie, W. R. Hansen, S. Sponberg, T. W. Kenny, R. Fearing, J. N. Israelachvili and R. J. Full, *Proc. Natl. Acad. Sci.*, 2002, **99**, 12252.
5 G. Huber, H. Mantz, R. Spolenak, K. Mecke, K. Jacobs, S. N. Gorb and E. Arzt, *Proc. Natl. Acad. Sci.*, 2005, **102**, 16293.
6 K. Autumn, Y. A. Liang, S. T. Hsieh, W. Zesch, W. P. Chan, T. W. Kenny, R. Fearing and R. J. Full, *Nature*, 2000, **405**, 681.
7 G. Walker, *Int. J. Adhes. Adhes.*, 1993, **13**, 3.
8 B. N. J. Persson, *J. Phys.: Condens. Matter*, 2007, **19**, 376110.
9 J. S. Wexler, T. M. Heard and H. A. Stone, *Phys. Rev. Lett.*, 2014, **112**, 066102.
10 S. Herminghaus, *Adv. Phys.*, 2005, **54**, 221.
11 A. Grimaldi, M. George, G. Pallares, C. Marlière and M. Ciccotti, *Phys. Rev. Lett.*, 2008, **100**, 165505.
12 A. F. G. Dixon, P. C. Croghan and R. P. Gowing, *J. Exp. Biol.*, 1990, **152**, 243.
13 T. Eisner and D. J. Aneshansley, *Proc. Natl. Acad. Sci.*, 2000, **97**, 6568.
14 S. N. Gorb, *Proc. R. Soc. London, Ser. B*, 1998, **265**, 747.
15 B. N. J. Persson, *J. Phys.: Condens. Matter*, 2008, **20**, 315007.
16 R. F. Shepherd, F. Llievski, W. Choi, S. A. Morin, A. A. Stokes, A. D. Mazzeo, X. Chen, M. Wang and G. M. Whitesides, *Proc. Natl. Acad. Sci.*, 2011, **108**, 20400.
17 H. J. Butt, W. J. P. Barnes, A. del Campo, M. Kappl and F. Schönfeld, *Soft Matter*, 2010, **6**, 5930.
18 H. Gao, B. Ji, I. L. Jäger, E. Arzt and P. Fratzl, *Proc. Natl. Acad. Sci.*, 2003, **100**, 5597.
19 R. W. Style, C. Hyland, R. Boltyanskiy, J. S. Wettlaufer and E. R. Dufresne, *Nat. Commun.*, 2013, 4.
20 F. London, *Trans. Faraday Soc.*, 1937, **33**, 8.
21 H. Hertz, *J. Reine Angew. Math.*, 1881, **92**, 110.
22 K. L. Johnson, K. Kendall and A. D. Roberts, *Proc. R. Soc. London, Ser. A*, 1971, **324**, 301.
23 T. Zhang, Z. Zhang, K. S. Kim and H. Gao, *J. Adhes. Sci. Technol.*, 2014, **28**, 226.
24 K. R. Shull and C. Creton, *J. Polym. Sci., Part B: Polym. Phys.*, 2004, **42**, 4023.
25 T. Yamaguchi, K. Koike and M. Doi, *Europhys. Lett.*, 2007, **77**, 64002.
26 J. Nase, C. Creton, O. Ramos, L. Sonnenberg, T. Yamaguchi and A. Lindner, *Soft Matter*, 2010, **6**, 2685.

27 R. W. Style, R. Boltyanskiy, Y. Che, J. S. Wettlaufer, L. A. Wilen and E. R. Dufresne, *Phys. Rev. Lett.*, 2013, **110**, 066103.
28 S. Mora, T. Phou, J. M. Fromental, L. M. Pismen and Y. Pomeau, *Phys. Rev. Lett.*, 2010, **105**, 214301.
29 A. Marchand, S. Das, J. H. Snoeijer and B. Andreotti, *Phys. Rev. Lett.*, 2012, **109**, 236101.
30 S. Das, A. Marchand, B. Andreotti and J. H. Snoeijer, *Phys. Fluids*, 2011, **23**, 072006.
31 B. Roman and J. Bico, *J. Phys.: Condens. Matter*, 2010, **22**, 493101.
32 R. W. Style and E. R. Dufresne, *Soft Matter*, 2012, **8**, 7177.
33 A. I. Rusanov, *Colloid J.*, 1975, **37**, 614.
34 A. I. Rusanov, *J. Colloid Interface Sci.*, 1978, **63**, 330.
35 E. R. Jerison, Y. Xu, L. A. Wilen and E. R. Dufresne, *Phys. Rev. Lett.*, 2011, **106**, 186103.
36 P. G. De Gennes, F. Brochard-Wyart and D. Quéré, *Capillarity and Wetting Phenomena: Drops, Bubbles, Pearls, Waves*, Springer, 2004.
37 L. D. Landau and E. M. Lifshitz, Course of Theoretical Physics, *Theory of Elasticity*, 1986, vol. 7.
38 J. B. Bostwick, M. Shearer and K. E. Daniels, *Soft Matter*, 2014, DOI: 10.1039/c4sm00891j.
39 J. F. Padday, G. Pétré, C. G. Rusu, J. Gamero and G. Wozniak, *J. Fluid Mech.*, 1997, **352**, 177.
40 I. Martinez, *Eur. Space Agency, [Spec. Publ.], SP*, 1983, **191**, 267.